*R*esearch in
*A*stronomy and
*A*strophysics

A coarse-to-fine strategy for the registration of the multi-wavelength high-resolution solar images

Rui Wang[1] and Zhi Xu[2]

[1] School of Electronics and Information, Xi'an Polytechnic University, Xi'an 710048, China
[2] Yunnan Astronomical Observatory, Chinese Academy of Sciences, Kunming 650011, China; *xuzhi@ynao.ac.cn*

Abstract The registration of multi-wavelength high-resolution solar images is an important task in the research of solar physics. This paper proposed a coarse-to-fine strategy to realize the accurate registration of high-resolution photospheric images and chromospheric images observed by the New Vacuum Solar Telescope (NVST) whose field-of-view is about $2' \sim 3'$, and the spatial resolution can reach $0.1''$ after image reconstruction. In this strategy, the full-disk solar images with relatively lower resolution taken by other space- or ground-based telescopes are taken as transition images, and the Fourier-Merlin transform, Template matching and a local statistical information based algorithm are used in combination. After registration, the geometric transformation between multi-wavelength images of NVST are corrected at the level of sub-arcseconds, including the rotation, scaling and translation relations. Two sets of data observed in active regions (i.e., the NOAA 11982 and the NOAA 12673) are used to illustrate our method step by step. The result shows that the registration accuracy can reach less than $1''$. Moreover, this work also has facilitated the combination of high-resolution observations of NVST with the continuum, ultraviolet passbands and magnetic field observations of the Solar Dynamic Observation (SDO), which is highly beneficial to the multi-instrument joint measurement of solar activities.

Key words: instrumentation: detectors — methods: observational — techniques: image processing — Sun: general

1 INTRODUCTION

It is well known that the multi-wavelength solar images can reveal a wide variety of the morphologies of solar activities at different atmospheric layers, which is important for the study of the Sun (Zuccarello 2016). However, these images are usually observed by different instruments with different spatial resolution, orientation and different telescope mount systems (e.g., the Alt-Az or Equatorial telescopes). Thus, image registration is a crucial step at the beginning of the studies so as to achieve the spatial co-alignment of these multi-wavelength images. Image registration is one of the basic image processes to match two or more images of the same scene taken at different times, from different sensors, or even from different viewpoints and in other conditions geometrically. So far, there are a lot of developed image registration algorithms, which have been widely used in medicine, remote sensing and other fields (Wolberg & Zokai 2000; Kennedy & Cohen 2003). However, there are some specific difficulties in the registration of multi-wavelength solar images.

The multi-wavelength solar images can be divided into two categories: full-disk images with low spatial resolution (about $0.5''\backsim 2''$) and local images with high spatial resolution (often less than $0.2''$) that have a partial field-of-view of full disk. For the full-disk image, taken in different wavelengths by different instruments, it is relatively convenient to register them taking the advantage of the solar limb structures and the knowledge of observation information, such as pointing information, plate scale, observation time, etc. (DeRosa & Slater 2013; Yoshimura & Mckenzie 2015). In comparison, for the local solar image, particularly taken by the ground-based telescope, they often lack accurate position information. What is more, solar features usually present quite different morphologies in multi-wavelength and the reference is hard to find. As a result, the study of accurate registration methods for high-resolution multi-wavelength images is necessary. For a long time, it was carried out through simple cross-correlation or trial-and-error method by use of some typical solar features (e.g., sunspots, pore, chromospheric brightening struc-

tures) to accurately register the multi-wavelength high-resolution solar images (Hong et al. 2016). But that is quite inefficient and the registration precision is always low (greater than $1''$). Recently, with the development of solar fine structure research, the precise registration of solar images has made a lot of progress. Feng et al. (2012) proposed a sub-arcsecond image registration algorithm for low signal-to-noise ratio images to achieve the correlation alignment of single-wavelength solar images. Yue et al. (2015) suggested an approach based on information entropy and scale-invariant feature transform (SIFT) algorithm to improve the registration quality of single-wavelength solar images. Feng et al. (2018) adopted a method of combining local statistical information with control points matching to achieve high-precision registration between the photospheric images taken by ground-based telescope and taken by space-based telescope. Yang et al. (2018) used a scale-invariant feature point matching method to solve the registration problem of solar magnetic field images from different instruments. Ji et al. (2019) developed an automatic mapping approach to determine the position of local solar image on the helioprojective-cartesian coordinates using an improved SIFT algorithm. All these methods have greatly improved the accuracy of solar image registration. Nevertheless, they are aimed at images taken from single wavelength and cannot be directly used for the registration between multi-wavelength solar images.

The New Vacuum Solar Telescope (NVST) of the Fuxian Solar Observatory (FSO) is a new generation solar observation facility of China (Liu et al. 2014). One of its main scientific goals is to observe fine solar structures at different layers using multi-wavelengths, including Hα, TiO-band, G-band and Ca II H and K lines (Xu et al. 2014). The highest spatial resolution can achieve about $0.1''$ (the diffraction limit resolution) at TiO-band after image reconstruction. In this paper, we propose a coarse-to-fine strategy, in which different registration algorithms are combined to realize the accurate co-alignment of multi-wavelength images of NVST with the precision of sub-arcsecond. During the process, the full-disk solar images after coordinate calibration is used as transition images, and the Fourier-Merlin transform and Template matching algorithm are used to carry out an initial localization of each single wavelength image pairs with pixel-wise precision. In addition, a local statistical information based algorithm is applied to improve the registration precision to sub-pixel-wise.

The rest of this paper is organized as follows. In Section 2, the basic algorithm principles are introduced. Section 3 introduces the characteristics of the observation data. In Section 4, the registration steps and result analysis

are described in details. Section 5 gives the discussion and conclusions.

2 INTRODUCTION OF ALGORITHM PRINCIPLES

2.1 Fourier-Merlin Transform

The Fourier-Merlin (FM) transform based registration method was proposed by Chen et al. (1994). It is widely studied and used in image processing field (Ayyalasomayajula et al. 2011). In general, FM transform can be realized by performing a log-polar coordinate transformation followed by the Fourier transform. The core idea of the FM transform method is to convert the problem of image rotation and scaling to the translation problem in log-polar coordinates, taking the advantage of the Fourier transform properties. Supposing two images, reference image – $f_1(x, y)$, sensed image – $f_2(x, y)$, with rotation, scaling and translation relations, the geometric transformation between them can be represented as

$$f_2(x,y) = f_1(\Delta x + s(x\cos\varphi - y\sin\varphi), \Delta y + s(x\sin\varphi + y\cos\varphi)), \quad (1)$$

where, φ, s and $(\Delta x, \Delta y)$ are the rotation, scaling and translation parameters respectively. Hereafter, we denote these geometric relations as RST (Rotation, Scaling and Translation) transformation. Applying the Fourier transform to Equation (1), we have

$$F_2(u,v) = \frac{e^{-j2\pi(\Delta xu + \Delta yv)}}{s^2} F_1(\frac{u\cos\varphi + v\sin\varphi}{s}, \frac{-u\sin\varphi + v\cos\varphi}{s}), \quad (2)$$

where, the $F_1(u, v)$ and $F_2(u, v)$ is the Fourier transform of $f_1(x, y)$ and $f_2(x, y)$ respectively. Carrying out log-polar transformation for Equation (2), that is, $u = e^\rho \cos\phi$, $v = e^\rho \sin\phi$, and taking the magnitude of both sides of Equation (2), we obtain the equation:

$$|F_2(e^\rho\cos\varphi, e^\rho\sin\varphi)| = \frac{1}{s^2}|F_1(e^{\rho-\log s}\cos(\theta+\varphi), e^{\rho-\log s}\sin(\theta+\varphi))|. \quad (3)$$

Equation (3) is symbolized as follows:

$$M_1^{LP}(\rho, \phi) = \frac{1}{s^2} M_1^{LP}(\rho - \log s, \theta + \varphi), \quad (4)$$

where Equation (4) is called the FM transform.

The advantage of the FM transform method is the low complexity and computation cost of the algorithm, but the disadvantage is that the accuracy of the parameters estimation in sub-pixel level is not very good. In this paper, the FM transform is used to estimate the rough RST parameters between full-disk solar image and high-resolution solar image.

2.2 Template Matching

Template matching is an approach to determine the position of a given template in a source image with large size. It is widely used in the computer vision field such as motion estimation, target detection, feature tracking, image mosaic, etc. (Luo & Konofagou 2010; Smeulders et al. 2014). The most popular and effective way to realize the Template matching is Normalized Cross-correlation (NCC) based method. In the NCC-based method, the template is shifted pixel-by-pixel across the source image to evaluate the cross-correlation coefficient value at each position, and then an NCC matrix is formed, denoted by $\rho(x, y)$. The best location of the template in source image is the position corresponding to the index of the maximum NCC value ($\rho(x, y)_{max}$). Let $t(x, y)$ denote the template with the size $m \times n$, and $f(x, y)$ denote the source image with the size $M \times N$, where $m < M$ and $n < N$. Then, the NCC matrix is defined as

$$\rho(x, y) = \frac{\sum_{i=1}^{m-i} \sum_{j=1}^{n-i} f(x+i, y+j) t(i, j) - mn\bar{f}_{i,j}\bar{t}}{\left\{ (\sum_{i=1}^{m-i} \sum_{j=1}^{n-i} f^2(x+i, y+j) - mn\bar{f}_{i,j}^2)(\sum_{i=1}^{m-i} \sum_{j=1}^{n-i} t^2(i, j) - mn\bar{t}^2) \right\}^{1/2}}. \tag{5}$$

In Equation (5), $\bar{f}_{i,j}$ denotes the mean value of large target image $f(x, y)$ within the area of the template t shifted to (i, j) which is calculated by

$$\bar{f}_{i,j} = \frac{1}{mn} \sum_{x=i}^{i+m-1} \sum_{y=j}^{j+n-1} f(x, y) \tag{6}$$

Similarly, $\bar{t}$ is the mean value of the template $t(x, y)$, $0 \leq i \leq m-1, 0 \leq j \leq n-1, 0 \leq x \leq M-m, 0 \leq y \leq N-n$.

Due to the normalization, $\rho(x, y)$ is robust to different lighting conditions across the image and less sensitive to noise. But the main drawback is that the calculation of Equation (5) is computationally expensive. A relatively efficient way of calculating the NCC matrix is by using the Fast Fourier Transformation (FFT) to compute the cross-correlation value and then using sum-tables to perform the normalization (Hanebeck 2001). In our strategy, the NCC-based template matching is used to perform an initial estimation of the position of high-resolution solar image in the full-disk image with pixel-wise precision.

2.3 Local Statistical Information Based Algorithm

For the purpose of further improvement of registration accuracy obtained from FM transform method and Template matching, a local statistical information based algorithm is proposed here, in which, both reference image and sensed image are divided into the same number of subsets with equal size. The cross-correlation of each subset pair is calculated to determine the displacement of the subset pair. Then we can obtain the matched points of all subset pairs according these displacements. Finally, the control points (CPs) are selected from these match points with some criterion, which are used to calculate the fine RST transformation parameters.

3 OBSERVATIONS

The aim of this work is to realize the accurate registration of multi-wavelength high-resolution images observed by the imaging system of NVST. An active region NOAA 11982 observed on 2014 April 25 is used to demonstrate our registration method. The data sets used here include:

- **TiO/NVST**: High resolution photospheric images taken at the TiO-band (λ705.8 nm) by NVST (Fig. 1(a)). The field-of-view is about $74'' \times 74''$ (1860×1860 pixels). The pixel sample is $0.04''$ pixel^{-1}.
- **Hα/NVST**: High resolution chromospheric images taken at the Hα (λ656.3 nm) by NVST (Fig. 1(b)). The field-of-view is about $131'' \times 131''$ (810×810 pixels), which is almost two times larger than TiO/NVST image. The pixel sample is $0.163''$ pixel^{-1}.
- **SDO/HMI**: Full-disk photospheric image taken at the continuum by the Helioseismic and Magnetic Imager (HMI) on board SDO spacecraft (Fig. 1(c)). The image size is 4096×4096 pixels, and the pixel sample is about $0.5''$ pixel^{-1}.
- **GONG**: Full-disk Hα image taken by the Global Oscillation Network Group (GONG) (Fig. 1(d)). The image size is 2048×2048 pixels, and the pixel sample is about $1''$ pixel^{-1}.

4 REGISTRATION STEPS AND RESULT ANALYSIS

Generally speaking, the implementation of the coarse-to-fine registration strategy in this work consists of three stages. Stage 1: Coordination calibration of the full-disk solar image. It is aimed at carrying out accurate co-alignment between full-disk solar images of SDO/HMI and GONG by means of standard process along with some specific processing proposed in this paper. Stage 2: Accurate
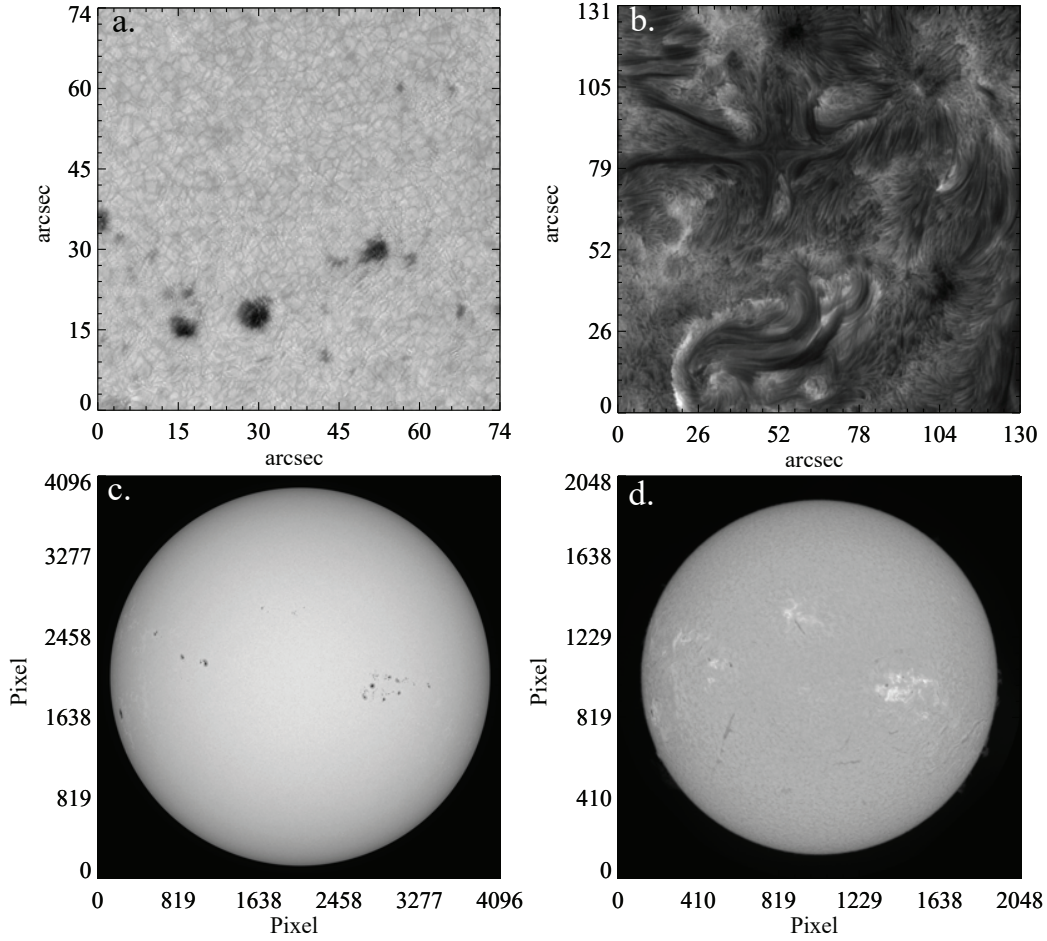
Fig. 1 Observations of the active region NOAA 11982 on 2014 April 25. (a) High-resolution photospheric observation at the TiO band observed by NVST. (b) High-resolution chromospheric observation at Hα line center obtained by NVST. (c) A full disk continuum image taken by the SDI/HMI. (d) A full disk chromospheric image provided by the GONG.

registration between high-resolution photospheric image and full-disk photospheric image. Using FM transform, the coarse co-alignment between them is realized. Afterwards, the local statistical information based method is carried out to obtain the fine registration between them. Stage 3: Accurate registration between high-resolution chromospheric image and full-disk chromospheric image. In this stage, the coarse registration step is implemented based on the Template matching algorithm, and then the local statistical information based method is used again to achieve the fine registration of the chromospheric images.

4.1 Stage 1: Accurate Co-alignment of Full-disk Solar Images

At the beginning, the GONG image is calibrated with reference to the SDO/HMI image coordinate system by using the SolarSoftWare IDL (SSWIDL) package (Brown et al. 2010). The calibration process includes a series of coordinate corrections, such as plate scales, roll angles, solar P-angle, solar East-West and North-South axes calibrations. Afterwards, it is found that there is still a certain systematic deviation with maximum value about 7 pixels (∼3.5″) near the solar limb. This systematic deviation may be caused by insufficient correction in the calibration of the solar P-angle (Hernandez et al. 2004; Hughes et al. 2013; Liang et al. 2017), and it is a rotational problem. Because the P-angle value in the header information of the GONG image is not very accurate, it is not fully corrected during coordinate calibration. Hence we propose to remove this deviation by calculating and correcting the residual rotation angle using large sunspot features. We firstly select sunspots on the full-disk solar images, which can be recognized in both the SDO/HMI images and GONG images, and then we use the center-of-gravity method to calculate the centroid of each sunspot. The rotation angle is calculated by

$$\theta = \sum_{i=1}^{N} \left(\arctan\left(\frac{y_i - y_c}{x_i - x_c}\right) - \arctan\left(\frac{y_i' - y_c}{x_i' - x_c}\right) \right) \Big/ N, \tag{7}$$
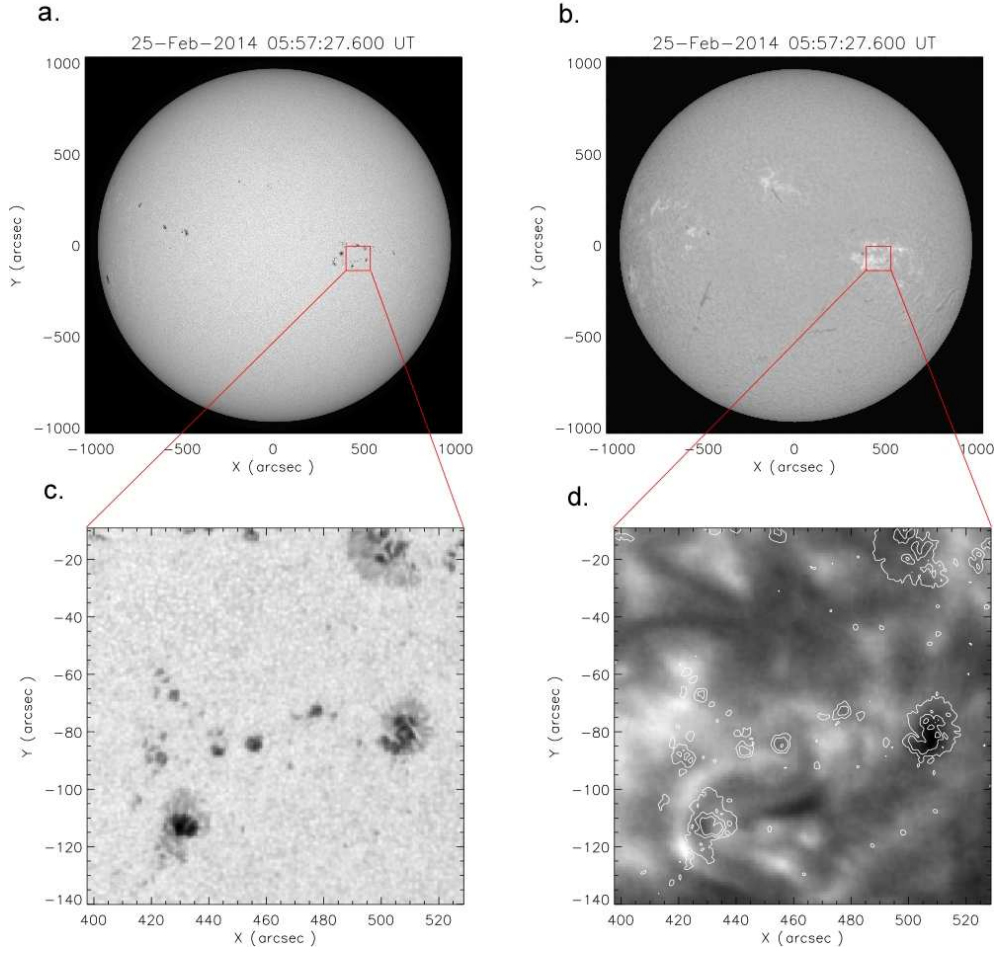
Fig. 2 Accurate co-alignment of the full-disk solar images. (a) SDO/HMI full-disk image used as the reference image. (b) The aligned GONG full-disk image. (c) SDO/HMI sub-image cut from the full-disk SDO/HMI image. (d) GONG sub-image cut from the full-disk GONG image, and the intensity contour of the SDO/HMI sunspot is over-plotted on the GONG sub-image showing the co-spatial of these two images.

where, the (x_c, y_c) denotes the solar disk center of SDO/HMI image. The (x_i, y_i) is the centroid of each sunspot in SDO/HMI image, and the (x'_i, y'_i) is the corresponding centroid of sunspot in GONG image. The rotation deviation is calculated to be $0.368°$ and is corrected. The alignment accuracy is quantitatively expressed by the root-mean-square error (RMSE), which is calculated to be 0.953 pixels ($0.476''$). The results are shown in Figure 2. Sub-regions, with field-of-view larger than NVST observations, are cut from the full-disk images based on the morphology of active region NOAA 11982 (see Fig. 2(c) and Fig. 2(d)).

4.2 Stage 2: Registration of Local Photospheric Images

Step 1: Coarse alignment: Based on the fact that there may be a large rotation and scaling relation between TiO/NVST image and SDO/HMI image, the initial registration between them is realized by FM transform method which is
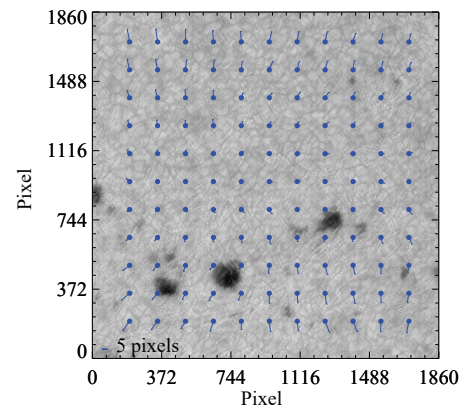
Fig. 3 The TiO/NVST image as the reference image is superposed by the CCPs (*blue dots*) and the corresponding cross-correlation displacement (*blue bars*) (*Color version is online*).

very suitable for this situation. Initially, the high-resolution TiO/NVST image is down-sampled to the magnitude of SDO/HMI image resolution. The $f_1(x, y)$ and $f_2(x, y)$
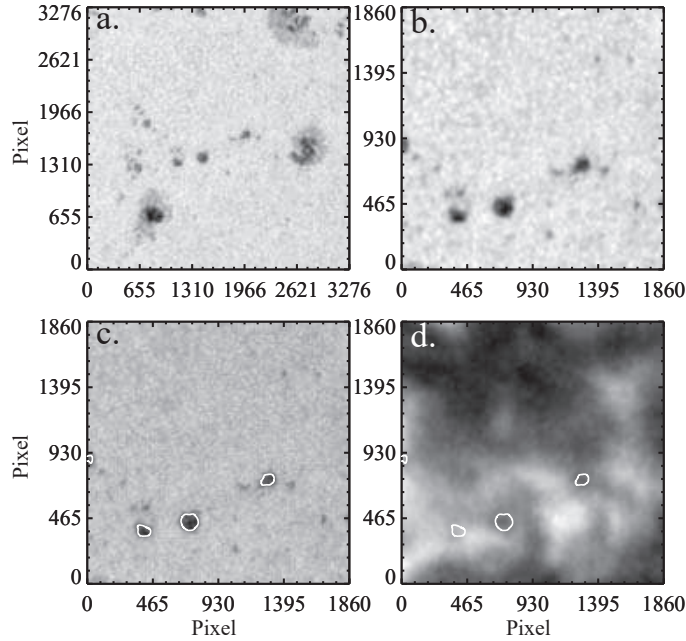
Fig. 4 The registration result between the full-disk image and TiO/NVST image. (a) A subregion taken from the SDO/HMI image before registration processing. (b) The SDO/HMI sub-image after fine alignment that has the same field-of-view as TiO/NVST image. (c) The TiO/NVST image with the sunspot intensity contours of the SDO/HMI sub-image after fine alignment over-plotted on it. (d) The aligned GONG sub-image superposed with the sunspot intensity contours of the SDO/HMI sub-image after the fine alignment.
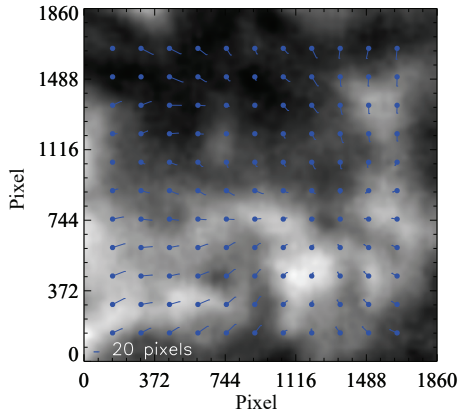
Fig. 5 The GONG sub-image as the reference image is superposed by the CCPs (*blue dots*) distribution and the corresponding cross-correlation displacements (*blue bars*).

in equation (Eq. (1)) correspond to the SDO/HMI sub-image and the down-sampled TiO/NVST image, respectively. Then, the coarse RST parameters are computed by FM transform method as: rotation is $0°$, scaling is 1.04, translation is (61,80) pixels. After that, the SDO/HMI sub-image is transformed according to these parameters, and another sub-region is cut which has almost the same field-of-view as TiO/NVST image. Meanwhile, the corresponding sub-region in GONG image is also cut. Finally, the coarsely aligned SDO/HMI sub-image and GONG sub-image are up-sampled to TiO/NVST resolution.

Step 2: Fine alignment: In this step, we refine the alignment accuracy by the registration method based on

local statistical information. The TiO/NVST image and SDO/HMI sub-image derived from step 1 are used to calculate the fine RST parameters with sub-pixel-wise precision. Firstly, both images are divided into 11×11 overlapping subsets with a size of 160×160 pixels. Secondly, the cross-correlation between each pair of subsets is calculated to determine the displacement between them. Only the displacements which are less than a specific threshold will be retained. The Cross-correlation Control Points (CCPs) pairs are obtained by using the centers of valid subset pairs and the corresponding displacements. Eventually, 121 CCPs pairs are obtained in this step. Figure 3 shows the locations of CCPs and displacements distribution. As we can see, these displacements present a systematic distribution. They are very symmetrical, pointing away from the center of the image, increasing from the center outward, and so on. It implies that there is still geometric misalignment between two images due to the insufficient alignment after FM transformation. Using these CCPs pairs, we construct the coordinate relation matrix and calculate the fine RST parameters by least square estimation (Wang et al. 2018). The fine RST parameters are as follows: rotation is $-0.1205°$, scaling is 0.991, translation is (3.117, 5.870) pixels. By using these RST parameters, a polynomial warping is performed to the SDO/HMI and GONG sub-images to realize the fine registration of these images. Figure 4 shows the final registration result of this stage.

After the final correction, we calculate the local cross-correlation displacements again. These displacements are

dramatically smaller than those before the final correction. We further calculate the RMSE of these non-zero displacements and regard it as the final registration accuracy in stage 2, which is 2.79 pixels (0.112″).

4.3 Stage 3: Registration of Local Chromospheric Images

Step 1: Coarse alignment: Since the large rotation and scaling have been corrected in stage 2, the NCC-based Template matching algorithm is used here to initially estimate the field-of-view location of the co-spatial GONG sub-image (i.e., the template) on Hα/NVST image (i.e., the source image) with pixel-wise precision. As a result, the origin of the GONG sub-image is located by Template matching at (567, 535) in Hα/NVST image.

Step 2: Fine alignment: At the beginning, Hα/NVST image co-spatial with GONG sub-image is cut out according to the initial location result of Step 1. Then, the registration method based on local statistical information is used again to refine the registration result to a high accuracy with sub-pixel-wise. Both images are divided into 11×11 overlapping subsets with a size of 230×230 pixels for each subset to calculate the local cross-correlation displacements. Figure 5 shows the displacement distributions of the CCPs pairs between the co-spatial Hα/NVST image and GONG sub-image. A number of 118 CCPs pairs are obtained to calculate the rotation, scaling and translation parameters to be –1.0191°, 1.0427, (–48.2284, –21.827) pixels, respectively. Again, a polynomial warping is performed to the coarse aligned Hα/NVST image by using these parameters, to realize the fine alignment. Figure 6 shows the final registration result of this stage. As shown in Figure 6(c), in order to demonstrate the alignment result, we over-plot the intensity contours of the Ha/NVST on the GONG image. We can see that contours outline the large scale bright features in the low resolution images well. The final registration RMSE accuracy of stage 3 is 11.74 pixels (0.470″).

4.4 Accuracy Analysis

In order to analyze the final registration accuracy of our method quantitatively, a compound RMSE is introduced. Considering the errors produced in the three main registration stages (i.e., the full-disk alignment RMSE ($\sigma_f = 0.476″$), local photospheric image alignment RMSE ($\sigma_p = 0.112″$) and local chromospheric image alignment RMSE ($\sigma_c = 0.470″$), the compound RMSE can be calculated, according to the theory of error transfer, by the following error transfer equation:

$$\sigma = \sqrt{\sigma_f^2 + \sigma_p^2 + \sigma_c^2}. \qquad (8)$$

Therefore, the final registration precision is $\sigma = 0.68″$.

4.5 Application to Solar Active Region NOAA 12673

Another active region NOAA 12673 were also well observed by NVST on 2017 September 5. Compared with the active region NOAA 11982 mentioned above, it harbors several mature sunspots. The umbra, light bridges and sheared penumbra are well exhibited in the TiO photospheric image of NVST, while quite different morphologies like loops and light patches present in the Hα chromospheric image. We apply our registration method to the multi-wavelength observations, including TiO/NVST photospheric image, Hα/NVST chromospheric images, the extreme ultraviolet (EUV) images and the magnetogram of SDO.

For the coarse registration of photospheric images, the RST parameters are calculated by FM transform as follows: rotation is 7.875°, scaling is 0.98, translation is (32, 38) pixels. At the step of fine registration of photospheric images, both images are divided into 121 subsets the same way as the above data set (NOAA 11982), and 121 CCPs pairs are obtained to calculated the fine RST parameters as: rotation is –0.0101°, scaling is 0.9874, translation is (5.3983, 12.776) pixels. Figure 7 shows the final result of the stage of local photospheric images registration. From Figure 7(c), we can see that the sunspot contour of SDO/HMI sub-image after fine registration has a good coincidence with the sunspot of TiO/NVST image. For the initial position estimation of chromospheric images, and the origin point coordinate of GONG sub-image is located at (219, 366) in Hα/NVST image. At the step of fine registration of chromospheric images, the images are divided into 121 subsets equally with a size of 320×320 pixels for each subset, and 108 valid CCPs pairs are obtained to determine the fine RST parameters to be as: rotation is $-0.3964°$, scaling is 1.003, translation is (–7.3152, 31.733) pixels. Figure 8 shows the final result of the stage of local chromospheric images registration. Figure 8(c) demonstrates the well co-space of the bright feature in Hα/NVST image and GONG image. Eventually, the final registration accuracy of the active region NOAA 11982 is computed as 0.97″.

Figure 9 shows the registration results of the active region NOAA 12673 image observed by NVST in TiO-band (Fig. 9(a)) and in Hα wavelength (Fig. 9(d)), along with the correspondence SDO/HMI sub-image after final registration (Fig. 9(b)), the vector magnetogram of SDO (Fig. 9(c)), and SDO/AIA sub-images in the 304 Å, 335 Å, 131 Å, 171 Å, 211 Å wavelength channels (Fig. 9(e)-(i)). The sunspot intensity of TiO/NVST image is contoured on itself, the SDO/HMI sub-images and magnetogram images respectively, which presents a good spatial relationship be-
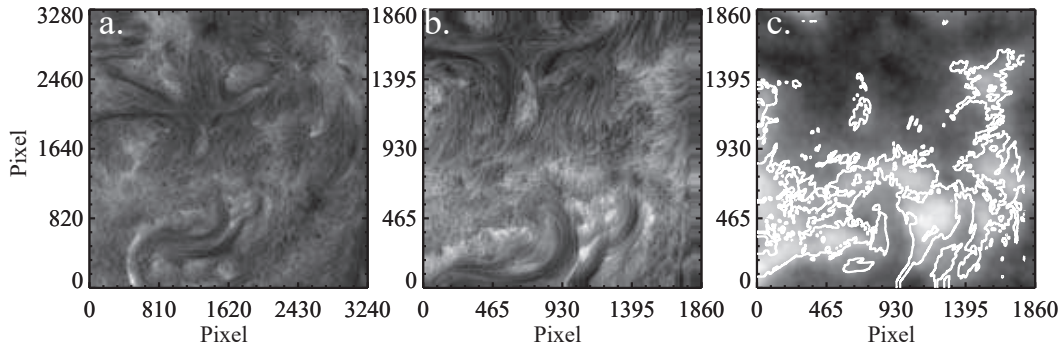
Fig. 6 The registration result between local chromospheric images. (a) The Hα/NVST image before registration. (b) The Hα/NVST image after fine alignment. (c) The GONG image with the bright region intensity contours of Hα/NVST after fine alignment over-plotted on it.
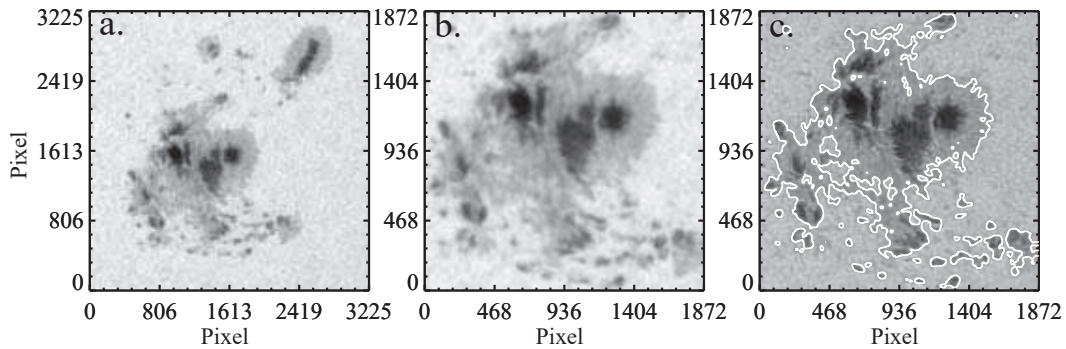
Fig. 7 The registration result between the full-disk and TiO/NVST images of the active region NOAA 12673. (a) A subregion taken from SDO/HMI image before registration processing. (b) The SDO/HMI sub-image after fine alignment which has the same field-of-view as TiO/NVST image. (c) The TiO/NVST image with sunspot intensity contours of SDO/HMI sub-image after fine alignment over-plotted on it.
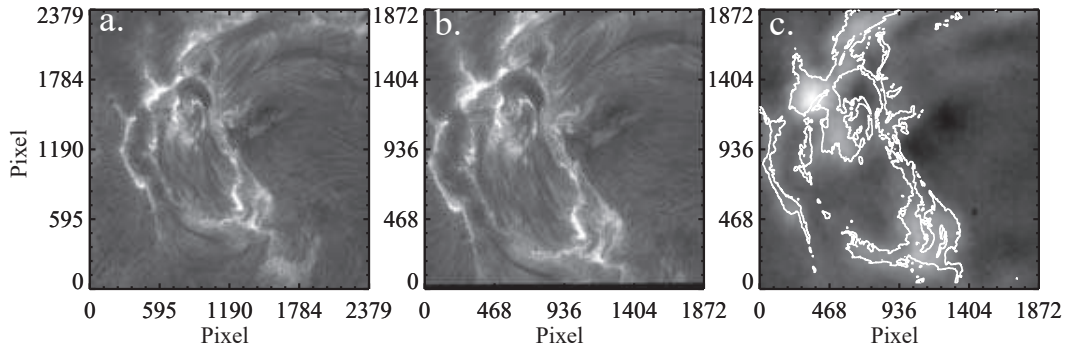
Fig. 8 The registration result between local chromospheric images of the active region NOAA 12673. (a) The Hα/NVST image before registration. (b) The Hα/NVST image after fine alignment. (c) The GONG sub-image with the bright region intensity contours of Hα/NVST after fine alignment over-plotted on it.

tween active phenomena and magnetic field. For example, we can see that the correspondence of bright bridge and the polar inverse line from Figure 9(c). Then the brightening structure intensity of Hα/NVST image is also contoured on itself and the EUV sub-images of SDO/AIA, which reflect a nice spatial correspondence between the high temperature brightening region in each SDO/AIA wavelength channel.

5 DISCUSSION AND CONCLUSIONS

In this paper, we have suggested a coarse-to-fine strategy to achieve precise registration of multi-wavelength solar images. Multiple algorithms, i.e., FM transform, Template matching, local statistical information based algorithm, are used in our method. By using this method, Hα/NVST image and TiO/NVST image are registered with a precision of less than 1″. This strategy not only solves the registration problem of solar images observed in different wave-
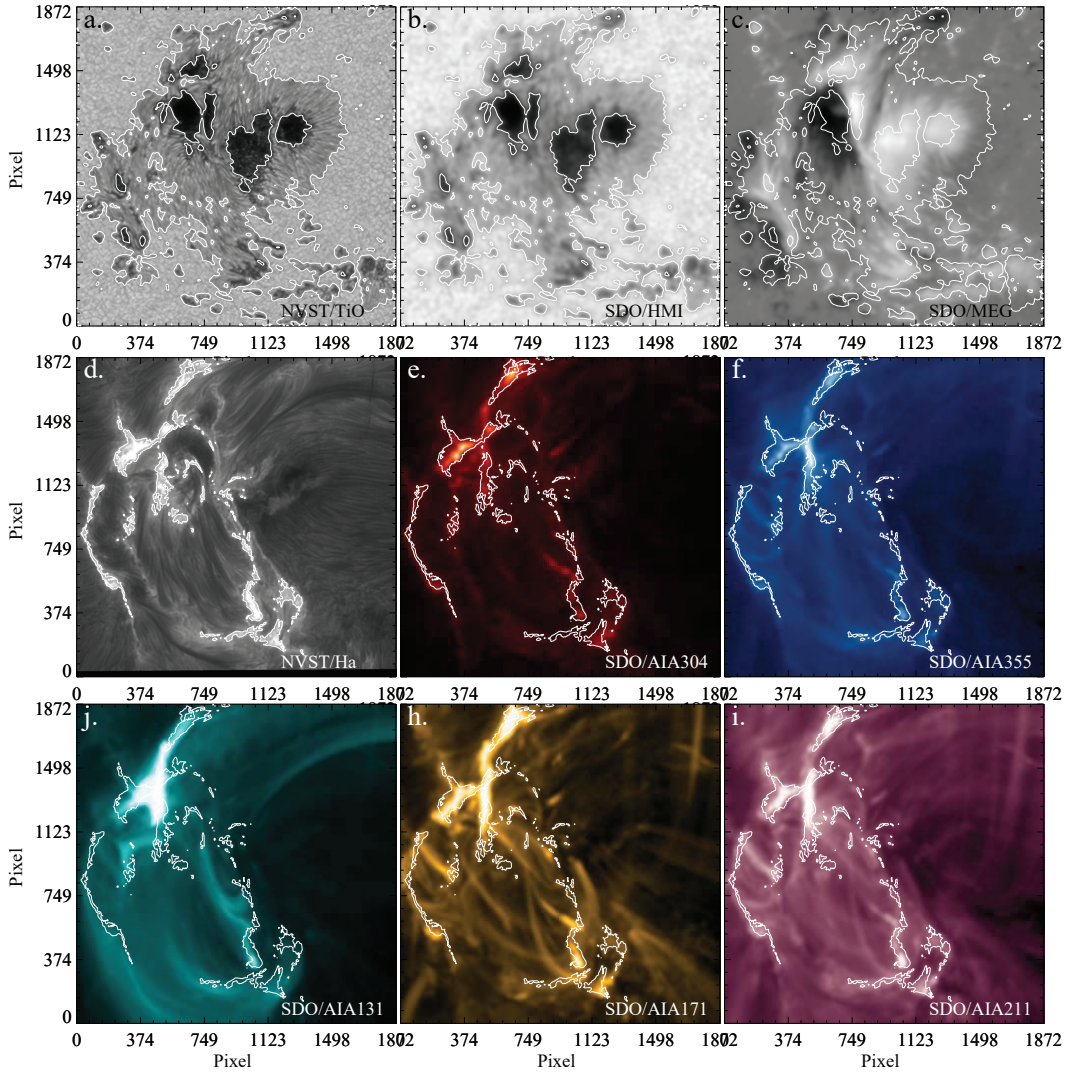
Fig. 9 The registered multi-wavelength images of NVST observations and SDO observations. (a) The reference TiO/NVST image; (b) the SDO/HMI sub-image after fine alignment. (c) The vector magnetogram of SDO after fine alignment. The sunspot intensity contours of TiO/NVST is over-plotted on these three images. (d) The Hα/NVST image after fine alignment. (e)-(i) The EUV sub-images of SDO/AIA in the 304 Å, 335 Å, 131 Å, 171 Å, 211 Å wavelength channels with the contours of the brightening region of Hα/NVST image after fine alignment over-plotted on them.

lengths by one piece of equipment (e.g., NVST), but also can realize the co-alignment of images taken by different equipments. It is very beneficial for the multi-instrument conjoint analysis of solar activity phenomena.

There are some important issues we should pay attention to during the registration process. That is the multi-wavelength observations, which often present different features or morphologies in different wavelengths. In this situation, the photospheric image (e.g., TiO/NVST image) cannot be directly aligned with the chromospheric image (e.g., Hα/NVST image), particulary in the observation of solar filaments, chromospheric fibers, or quiet region spicule, etc. Therefore, a "bridge" is needed as a transition to connect these images. We take the full-disk solar image observed in the similar wavelength as this bridge in our present work, which can be easily co-aligned accurately. As a result, the registration accuracy is certainly limited by the resolution of the full-disk solar image. Additionally, the number of the CCPs also plays an important role in the fine registration stage of our method. It relates to the field-of-view, resolution and signal-to-noise of solar images. The greater the number of CCPs the better the registration accuracy we can achieve. But it is needed to take care of the balance between the accuracy and time consumption of the algorithm. In case of NVST observations, we have found that about a hundred CCPs are enough for the accuracy of sub-arcsecond.

If there is no full-disk image available, a scheme of dense wavelength scan observation by use of the Lyot or Fabry-Perot filter system can be adopted. In that scheme,

each adjacent off-band image shows many quite similar features and can be exploited as the bridge, which will be studied in our further research. For the co-alignment of quiet atmosphere data where no sunspots or pores are observed by the high resolution local images, our method cannot work very well, since the weak-contrasted features (e.g., granules) cannot be recognized in the full-disk image clearly. For this case, we prefer to use the so-called optical calibration method, which is independent of the solar features. More details of the optical calibration method can be found in Wang et al. (2018).

References

Ayyalasomayajula, P., Grassi, S., & Farine, P. A. 2011, in 19th European Signal Processing Conference, IEEE, 769

Brown, D., Regnier, S., Marsh, M., et al. 2010, Working with data from the Solar Dynamics Observatory, STFC Advanced Summer School 2010

Chen, Q., Defrise, M., & Deconinck, F. 1994, IEEE Transactions on Pattern Analysis and Machine Intelligence, 16, 1156

DeRosa, M., & Slater, G. 2013, Lockheed Martin Solar & Astrophysics Laboratory, Palo Alto, CA

Feng, T., Dai, W., Wang, R., et al. 2018, Astronomical Research & Technology, 15(1), 69 (in Chinese)

Feng, S., Deng, L., Shu, G., et al. 2012, IEEE 5th Int. Conf. on Advanced Computational Intelligence (ICACI), 626, (New York: IEEE)

Hanebeck, U. D. 2001, in Proceeding of Spie on Optical Pattern Recognition XII, 4387, 95

Hernandez, I. G., Durney, B. R., Komm, R., et al. 2004, ApJ, 605, 554

Hong, J., Ding, M.-D., Li, Y., et al. 2016, ApJ, 820, L17

Hughes, A. L. H., & the NISP Interiors et al. 2013, Technical Report No. NSO/NISP-2013-004

Ji, K.-F., Liu, H., Jin, Z.-Y., et al. 2019, Chin Sci Bull, 64, 1738 (in Chinese)

Kennedy, R. E., & Cohen, W. B. 2003, International Journal of Remote Sensing, 24, 3467

Liang, Z.-C., Birch, A. C., Duvall, T. L., et al. 2017, A&A, 601, A46

Liu, Z., Xu, J., Gu, B.-Z., et al. 2014, RAA (Research in Astronomy and Astrophysics), 14, 705

Luo, J., & Konofagou, E. E. 2010, IEEE Transactions on Ultrasonics Ferroelectrics and Frequency Control, 57, 1347

Wang, R., Xu, Z., Chen, Y.-C., et al. 2018, Acta Optica Sinica, 38, 0111002 (in Chinese)

Smeulders, A. W. M., Chu, D.-M., Cucchiara, R., et al. 2014, IEEE Transactions on Pattern Analysis and Machine Intelligence, 36, 1442

Wolberg, G., & Zoka, S. 2000, in Proceedings of SPIE - The International Society for Optical Engineering

Xu, Z., Jin, Z.-Y., Xu, F.-Y., et al. 2014, in Proc. of IAU Symp., 300, 117

Yang, P., Zeng, S.-G., Liu, S., et al. 2018, Astronomical Research & Technology, 15, 59 (in Chinese)

Yue, X., Shang, Z.-H., Qiang, Z.-P., et al. 2015 Computer Science, 42, 57 (in Chinese)

Yoshimura, K., & Mckenzie, D. 2015, Solar Physics, 290, 2355

Zuccarello, F. 2016, Astronomische Nachrichten, 337, 1070